ELSEVIER

Biophysical Chemistry 64 (1997) 199–209

Biophysical Chemistry

Regulation of rabbit muscle phosphofructokinase by phosphorylation

Guang-Zuan Cai [a], Thomas P. Callaci [a], Michael A. Luther [b], J. Ching Lee [c,*]

[a] *E.A. Doisy Department of Biochemistry and Molecular Biology, St. Louis University School of Medicine, St. Louis, MO 63104, USA*
[b] *Glaxo Research Institute, Research Triangle Park, NC 27709, USA*
[c] *Department of Human Biological Chemistry and Genetics, The University of Texas Medical Branch, Galveston, TX 77555-1055, USA*

Received 26 July 1996; revised 5 September 1996; accepted 5 September 1996

Abstract

Muscle phosphofructokinase is one of the glycolytic enzymes whose partitioning between the particulate and soluble fractions in skeletal muscle is linked to the biological activity of the muscle. The formation of the enzyme–actin complex is apparently regulated by phosphorylation of the enzyme. In order to understand the role of phosphorylation on the regulatory mechanism of phosphofructokinase, the self-association of the phosphorylated and dephosphorylated forms of phosphofructokinase was studied by investigating the sedimentation velocity at pH 7.0 and 23°C in different solvent constituents. The results show that both the phosphorylated and dephosphorylated forms of the enzyme exhibit the same mechanism of assembly. The effects of allosteric effectors are dependent on the phosphorylation state of the enzyme. The presence of 0.2 mM fructose-6-phosphate, one of the two substrates, leads to a significant enhancement in the formation of octomers without altering the equilibrium constant for tetramerization for either phosphorylated or dephosphorylated enzyme. The presence of 10 mM citrate, an allosteric inhibitor, leads to the formation of a significant amount of dimer, an inactive form of the enzyme. Citrate decreases the propensities of the dephosphorylated and phosphorylated forms of the enzyme to tetramerize 3000 times and 100 times, respectively. Based on the mode of subunit assembly, bimodal sedimentation velocity profiles can be obtained by simulation. Furthermore, simulation showed that the seemingly very different profiles reported in the literature can be accounted for by various combinations of equilibrium constants. In summary, this study showed that the propensity of subunit assembly is affected differentially by specific metabolites and the phosphorylation state of phosphofructokinase.

Keywords: Phosphorylation; Self-association; Allosteric regulation; Protein–protein interaction; Phosphofructokinase

1. Introduction

In skeletal muscles, the structural proteins seem to be the site for reversible binding of glycolytic enzymes [1–3]. Such reversible complex formation may play a significant role in the metabolic control mech-

Abbreviations: PFK, rabbit muscle phosphofructokinase; GKMED buffer, 65 μM glycylglycine buffer with 10 mM KCl, 15 mM $MgCl_2$, 1 mM EDTA and 1 mM DTT at pH 7.0; TEMA buffer, 25 mM Tris-CO_3 buffer with 1 mM EDTA, 6 mM $MgCl_2$ and 30 mM $(NH_4)_2SO_4$ at pH 7.0

* Corresponding author.

PII S0301-4622(96)02232-6

anism, since the skeletal muscle proteins can serve as the support for the enzyme–enzyme interaction which in turn leads to metabolic transfer [4,5].

The interaction between skeletal muscle proteins and glycolytic enzymes is sensitive to the pH, ionic strength and concentration of metabolites [6,7]. One of the glycolytic enzymes that has been shown to be reversibly associated with filamentous actin is muscle phosphofructokinase [8–11]. The partitioning of muscle phosphofructokinase between the particulate and soluble fractions is apparently intimately linked to the biological activity of the muscle. The enzyme is found in higher abundance in the particulate fraction of stimulated muscle, whereas in unstimulated muscle, it is present mostly in the cytosol [12,13]. The formation of an enzyme–actin complex affects the steady-state kinetic behavior of PFK [8,14]; hence, it seems that actin can serve as a positive effector for PFK activity.

The formation of the PFK–actin complex is regulated by the phosphorylation of PFK [8,9]. The phosphorylated form of the enzyme demonstrates a higher affinity for F-actin than the dephosphorylated form. Steady-state kinetic measurements show that F-actin acts as an effector of the phosphorylated form but does not significantly affect the dephosphorylated form. Results from these in vitro studies are consistent with in vivo observations that phosphorylation of PFK is directly proportional to the stimulation of muscle contraction; thus, this post-translational modification of PFK may serve as a means to regulate the compartmentalization of the enzyme in order to provide energy to the cellular component where it is needed.

It is evident that the localization and regulation of PFK is intimately linked to post-translational modification; however, the regulation of enzyme activity is also modulated by subunit assembly [15–20]. The enzyme can undergo a dynamic reaction of subunit association–dissociation in the mode monomer $\rightleftarrows$ tetramer, in which the tetramer is the active form. Since F-actin serves as an activator of PFK, the formation of the PFK–actin complex most likely affects the equilibrium of the subunit assembly by favoring the formation of active tetramer. As the linkages among post-translational modification and macromolecular assembly are important in the regulation of muscle PFK, it is imperative that these linkages of the multiequilibria be quantitatively defined.

Based on present knowledge, the identified equilibria can be linked by the following simple scheme

$$\begin{array}{ccc} E_4' + A & \rightleftarrows & E_4'A \\ \uparrow\downarrow & & \uparrow\downarrow \\ E_1' + A & \rightleftarrows & E_1'A \\ P_i \updownarrow & & \updownarrow P_i \\ E_1 + A & \rightleftarrows & E_1A \\ \uparrow\downarrow & & \uparrow\downarrow \\ E_4 + A & \rightleftarrows & E_4A \end{array}$$

where E_i and E_i' are the dephosphorylated and phosphorylated forms of PFK, respectively, $i = 1$ or 4 is the number of PFK subunits in that particular enzyme species, A is actin, and E_iA and $E_i'A$ are the PFK–actin complexes of the dephosphorylated and phosphorylated forms of PFK, respectively. Based on this simple scheme, it is evident that the need to characterize the various equilibria that govern the linkage scheme is real; thus, it is important to determine independently the association constants of the phosphorylated and dephosphorylated forms of PFK. In addition, the formation of an enzyme–actin complex establishes a thermodynamic linkage between the two self-assembly systems, i.e. enzyme subunit assembly and G-actin assembly. It is useful to characterize the effect of enzyme on the self-assembly of G-actin. In this study, the effect of phosphorylation on PFK assembly is quantitated, the effects of solvent composition probed and the actin assembly process in the presence of PFK is monitored.

2. Materials and methods

ATP, F6P, DTT, the catalytic subunit of the 3′, 5′ cAMP-dependent protein kinase, and bovine intestine alkaline phosphatase, type VII, were purchased from Sigma Chemical Company. Aldolase, glycerol-3-phosphate dehydrogenase/triose phosphate isomerase, and NADH were obtained from Boehringer (Mannheim, Germany). These were all used without further purification. PFK was purified, stored, and assayed as previously described [19].

In vitro phosphorylation of PFK was accomplished by the procedure reported by Kitajima et al. [21], and adopted by Luther and Lee [8]. PFK was dephosphorylated by the method of Foe and Kemp [22] as reported by Luther and Lee [8]. The amount of phosphate covalently bound to PFK was determined by the procedure of Hasegawa et al. [23], using phosphoserine as the standard.

Protein concentrations were determined spectrophotometrically. The wavelength and adsorptivity coefficient are 280 nm and 1.07 l g^{-1} cm^{-1}, respectively, for PFK [15].

In all experiments, PFK was equilibrated in the appropriate buffer by passage through a Sephadex G-25 column (1.2 cm × 8.5 cm). PFK was assayed for its activity and regulatory properties as previously described [8].

Sedimentation velocity studies were performed and the results analyzed by published procedures [15]. Weight-average sedimentation coefficients were normalized to standard conditions by correcting for the solvent density and viscosity. Experiments were performed in one of three buffer systems at pH 7.0 and 23°C: GKMED buffer, TEMA buffer and 3 × TEMA buffer. For all the experiments, Kel-F coated aluminum double-sector centerpieces with sapphire windows were used. The apparent partial specific volume of PFK is 0.730 [16].

The formation of F-actin from G-actin in the presence or absence of PFK was followed by turbidity [24]. The assembly buffer consisted of the same buffer used in the kinetic and self-association studies. The turbidity was measured at 350 nm in a Gilford 250 recording spectrophotometer. Protein solutions were initially incubated at 10°C in a cuvette which was thermostatically regulated by a Gilford thermostatic cuvette holder. Assembly of F-actin was initiated by the addition of 0.1 ml of 65 μM glycylglycine, 150 mM $MgCl_2$, 100 mM KCl, 1 mM EDTA, and 1 mM DTT at pH 7.0 to a 0.9 ml solution of actin in 65 μM glycylglycine, 1 mM EDTA and 1 mM DTT at pH 7.0, such that the final concentrations of $MgCl_2$ and KCl were 15 mM and 10 mM, respectively. The reversibility of F-actin formation was demonstrated by an increase and decrease in turbidity at 37°C and 10°C, respectively. The equilibrium constant for F-actin assembly, K_p^{app}, was obtained from the turbidity data as the reciprocal of the critical concentration, assuming that the condensation theory of Oosawa and Kasai [25] can describe adequately the polymerization process of actin.

3. Results

The amount of phosphate covalently bound to PFK is (0.09 ± 0.008) mole phosphate per mole of subunit. This is the maximum amount of phosphorylation regardless of the duration of the in vitro phosphorylation reaction. Maximum phosphorylation was reached in less than 1 h and routinely the reaction was allowed to proceed for 2 h. These results are in good agreement with the reports of one phosphate group per PFK monomer [21,22]. The dephosphorylation reaction is very efficient since there is no detectable amount of phosphate left after alkaline phosphatase treatment as indicated by an experimentally determined content of (0.01 ± 0.01) mole phosphate per mole of subunit.

The effect of phosphorylation on PFK subunit assembly was investigated in three different buffer systems that have been employed in various aspects of the study in this laboratory. The sedimentation behavior of PFK was studied as a function of protein concentration for both the phosphorylated and dephosphorylated forms in these buffer systems. In this study, as in all earlier studies in this laboratory, the systems were tested for rapid, dynamic equilibrium by reference to the measurement of $\bar{S}_{20,w}$ as a function of the number of revolutions per minute and the independence of $\bar{S}_{20,w}$ as a function of the time of dilution from a stock solution of higher protein concentration. Results in 3 × TEMA are reported in order to illustrate typical observations from these tests. First, a 300 μg ml^{-1} solution of phosphorylated PFK was subjected to sedimentation velocity analysis at 40000 and 60000 rev min^{-1}. $\bar{S}_{20,w}$ values of (13.9 ± 0.2)S and (13.8 ± 0.2)S were obtained at low and high speed, respectively. Second, a concentrated stock solution of 5 mg ml^{-1} was diluted to 300 μg ml^{-1} and the diluted sample was subjected to sedimentation velocity analysis at 60000 rev min^{-1} as a function of the time after dilution at 2 h intervals. Identical $\bar{S}_{20,w}$ values of (13.8 ± 0.2) were obtained for samples after 0–4 h of dilution,

indicating the absence of a slow equilibrium such as for a non-interacting, denatured component. For samples in 3 × TEMA buffer, a third test was conducted. It involves the fractionation of a PFK sample of 5 mg ml^{-1} by sedimentation using an aluminum partition centerpiece. The leading and trailing fractions are those that have or have not passed the partition, respectively. The two fractions were isolated and diluted to the same protein concentration as for the unfractionated PFK. The three samples of 400 μg ml^{-1} of PFK were then subjected to sedimentation velocity studies. The observed values for $\bar{S}_{20,w}$ are 14.8, 14.7 and 14.6 for the trailing, leading and unfractionated samples, respectively. Thus, in all cases, these tests yielded results that indicated the presence of a system in rapid, dynamic equilibrium. Typical results in GKMED and 3 × TEMA buffer systems are shown in Fig. 1A and 1B, respectively. In GKMED, a difference between the phosphorylated and dephosphorylated forms in their propensity to aggregate is observed, whereas in the 3 × TEMA buffer system, this difference is suppressed.

The sedimentation data are further analyzed in accordance with

$$\bar{S} = \sum_i S_i^\circ (1 - g_i C) K_i C_1^i / \sum_i K_i C_1^i \qquad (1)$$

where S_i° is the sedimentation coefficient of the ith species at infinite dilution, g_i is the non-ideality coefficient, $C = \sum_i K_i C_1^i$, K_i is the equilibrium constant between any i-mer and the monomer, and C_1 is the monomer concentration. The various S_i° values used in the fitting are $S_1^\circ = 5.4S$, $S_2^\circ = 8.5S$, $S_8^\circ = 21.4S$ and $S_{16}^\circ = 34.0S$. The rationale for and validity of adopting these values have been discussed [26]. If multiple modes seem to fit the data, the same set of rules as described previously is adopted in order to determine the appropriate stoichiometry and equilibrium constants [26]. Briefly, mode(s) of the lowest standard root mean square deviation (σ) or sum of squares of residuals (SS) are chosen. The mode with the smallest number of species will be chosen among those with similar σ or SS.

The sedimentation data for both the phosphorylated and dephosphorylated forms of PFK were analyzed for different modes of association. The results are summarized in Table 1. It is evident that the mode that contains the species of M_1, M_4 and M_8

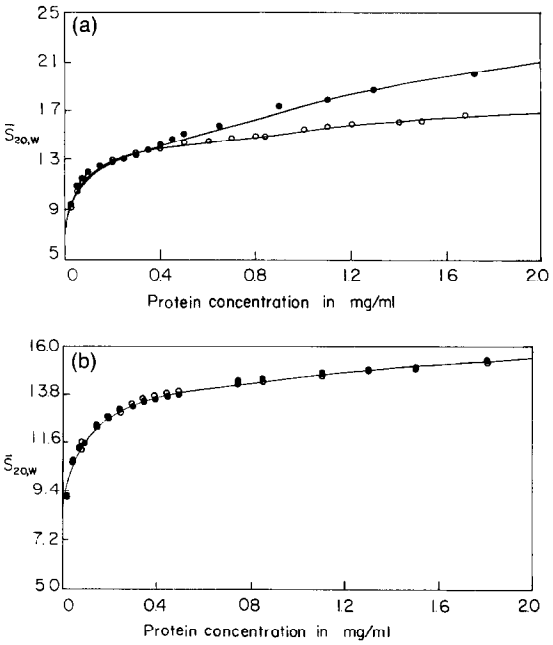

Fig. 1. (A) Relationship between the weight-average sedimentation coefficient and the PFK concentration in GKMED buffer at pH 7.0 and 23°C. ●, phosphorylated PFK; ○, dephosphorylated PFK. The lines represent the theoretical fit of the experimental data with the association model of $M_1 \rightleftharpoons M_4 \rightleftharpoons M_8 \rightleftharpoons M_{16}$. The data points represent the average of multiple data sets. (B) Relationship between the weight-average sedimentation coefficient and the PFK concentration in 3×TEMA buffer at pH 7.0 and 23°C. The symbols and conditions are the same as (A).

best describes all the data sets. In the presence of three times the TEMA, the values of K_i are similar to that of the dephosphorylated form in GKMED buffer. These results imply that with respect to its propensity to self-aggregate, under these experimental conditions, only the phosphorylated form of PFK is sensitive to the solvent environment whereas the dephosphorylated form is less or not responsive.

The relationship between $\bar{S}_{20,w}$ and the protein concentration reveals not only the stoichiometry of the reaction but also the ratio of the equilibrium constants characterizing these linked multiple equilibria. Intuitively, one may expect to observe a steeper relationship between $\bar{S}_{20,w}$ and the protein concentration if the value of K_i is increased. Why, then, do the results in Fig. 1 show a shallower relationship with larger values of K_i, as in the case of dephos-

Table 1
Summary of fitting for weight-average sedimentation data at pH 7.0 and 23°C

Stoichiometry/composition	K_2 (ml mg^{-1})	K_4 (ml mg^{-1})^3	K_8 (ml mg^{-1})^7	K_{16} (ml mg^{-1})^{15}	*SS*
GKMED buffer					
A. Phosphorylated PFK					
1:4:16	–	$(4.2 \pm 3.0) \times 10^5$	–	$(1.7 \pm 5.9) \times 10^{22}$	184
1:2:4:1	(5 ± 8)	$(1.7 \pm 0.2) \times 10^5$	–	$(4.6 \pm 4.8) \times 10^{20}$	187
1:4:8:16	–	$(6.2 \pm 0.3) \times 10^4$	$(3.5 \pm 0.4) \times 10^9$	$(3.9 \pm 0.7) \times 10^{19}$	15
1:2:4:8:16	(44 ± 5)	$(2.0 \pm 0.2) \times 10^5$	$(7.1 \pm 0.8) \times 10^{10}$	$(8.9 \pm 1.2) \times 10^{21}$	20
B. Dephosphorylated PFK					
1:4:16	–	$(8 \pm 6) \times 10^5$	–	$(1.5 \pm 2) \times 10^{23}$	126
1:2:4:16	(1 ± 25)	$(6.5 \pm 0.2) \times 10^5$	–	$(5.6 \pm 3.4) \times 10^{22}$	126
1:4:8:16	–	$(1.2 \pm 0.2) \times 10^5$	$(2.1 \pm 0.5) \times 10^{10}$	$(8.8 \pm 5.0) \times 10^{19}$	5.4
1:2:4:8:16	(3.7 ± 7.0)	$(1.3 \pm 0.5) \times 10^5$	$(2.7 \pm 2.6) \times 10^{10}$	$(9.3 \pm 10.7) \times 10^{19}$	6.5
TEMA buffer [a]					
A. Phosphorylated PFK	–	$(3.7 \pm 0.4) \times 10^5$	$(6.3 \pm 2) \times 10^{10}$	$(1.7 \pm 0.4) \times 10^{22}$	5.0
+ 10mM citrate	(7 ± 2)	$(3.7 \pm 0.8) \times 10^3$	$(5.5 \pm 1.6) \times 10^6$	–	6.3
+ 0.2mM F6-P	–	$(1.4 \pm 0.7) \times 10^5$	$(4.6 \pm 2.5) \times 10^{12}$	–	2.4
B. Dephosphorylated PFK	–	$(2.6 \pm 0.3) \times 10^5$	$(3.7 \pm 0.3) \times 10^{10}$	$(4.2 \pm 2) \times 10^{20}$	2.0
+ 10mM citrate	(36 ± 8)	(92 ± 5)	$(5 \pm 5) \times 10^6$	–	7.9
+ 0.2mM F6P	–	$(2.0 \pm 0.3) \times 10^5$	$(3.6 \pm 0.8) \times 10^{11}$	$(2.4 \pm 1.1) \times 10^{22}$	9.3
3xTEMA buffer					
Phosphorylated/dephosphorylated PFK					
1:4:16	–	$(1.2 \pm 0.1) \times 10^6$	–	$(8.5 \pm 2.6) \times 10^{22}$	35
1:4:8	–	$(3.3 \pm 0.1) \times 10^5$	$(4.5 \pm 0.3) \times 10^{10}$	–	1.1
1:2:4:8	(6 ± 2)	$(3.8 \pm 0.2) \times 10^5$	$(6.1 \pm 0.9) \times 10^{10}$	–	0.9

[a] The data obtained in TEMA buffer alone are from Cai et al. [26]. The mode of association in 0.2mM F6-P remains the same as $M_1 \rightleftharpoons M_4 \rightleftharpoons M_8 \rightleftharpoons M_{16}$ but the values of S_i° are $S_1^\circ = 5.4S$, $S_4^\circ = 12.4S$, $S_8^\circ = 19.7S$ and $S_{16}^\circ = 31.3S$. The mode of association in 10 mM citrate is $M_1 \rightleftharpoons M_2 \rightleftharpoons M_4$ and the values of S_i° are the same as in the buffer alone.

phorylated PFK? In order to address this issue, a detailed analysis of the effects of K_i values on the relationship between $\bar{S}_{20,w}$ and the protein concentration was conducted. The results of this study are shown in Fig. 2. In Fig. 2A, the only variable is K_4. After an initial steep increase in $\bar{S}_{20,w}$, the slope of $\bar{S}_{20,w}$ versus concentration actually decreases with increasing K_4. In Fig. 2B, the variable parameter is K_8. At concentrations below 1 mg ml^{-1}, the slope of $\bar{S}_{20,w}$ versus concentration increases with increasing values of K_8. However, at about 1.3 mg ml^{-1}, these lines actually cross over each other. In Fig. 2C, the variable parameter is K_{16}. In contrast to the earlier observations, the slope of $\bar{S}_{20,w}$ versus concentration increases with increasing K_{16}. Thus, the shape of the relationship between $\bar{S}_{20,w}$ and protein concentration is a complex function of stoichiometry and ratio of the equilibrium constants. The change in shape of the curve describing $\bar{S}$ vs. C may sometimes be different from that predicted by intuition.

Knowing the mode of association and the equilibrium constants, it is possible to calculate for the distribution of species as a function of total protein concentration. The weight percent distribution of various species in GKMED buffer is shown in Fig. 3A and 3B. It is evident that at protein concentrations below 20 μg ml^{-1}, the predominant species is monomeric PFK for either the phosphorylated or dephosphorylated form. Tetrameric and octameric species become the major ones at higher concentrations; however, even at these higher concentrations the distribution of the 16-mer still has not become the dominant species. The data in the 3 × TEMA buffer were similarly analyzed and the results are shown in Fig. 3C. In this case, species greater than the tetramer are not present in a significant amount

until the total protein concentration is greater than 100 μg ml^{-1}.

Since most of the steady-state kinetic studies from this laboratory were conducted in TEMA buffer, it would be interesting to evaluate the effect of substrate, F6-P, and inhibitor, citrate, on the subunit assembly of phosphorylated and dephosphorylated PFK in this TEMA buffer system. The results of these studies are summarized in Table 1. In the presence of 0.2 mM F6-P, the sedimentation data can be best fitted only if the sedimentation coefficients $S_1°$, $S_4°$, $S_8°$ and $S_{16}°$ assume values of 5.4, 12.4, 19.7 and 31.3, respectively. These observations are

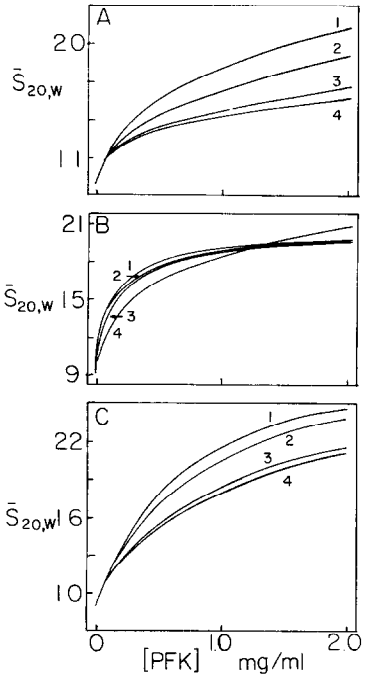

Fig. 2. Simulated relationships of $\bar{S}_{20,w}$ and the PFK concentration. The mode of association is $M_1 \rightleftharpoons M_4 \rightleftharpoons M_8 \rightleftharpoons M_{16}$. (A) Relationships for constant K_8 and K_{16} but varying K_4; $K_8 = 2 \times 10^9$ (ml mg^{-1})^7 and $K_{16} = 6 \times 10^{18}$ (ml mg^{-1})^{15}. The symbols and values of K_4 (ml mg^{-1})^3 are (1) 4×10^4, (2) 6×10^4, (3) 9×10^4, and (4) 1.1×10^5. (B) Relationships for constant K_4 and K_{16} but varying K_8; $K_4 = 6 \times 10^4$ (ml mg^{-1})^3 and $K_{16} = 6 \times 10^{18}$ (ml mg^{-1})^{15}. The symbols and values of K_8 (ml mg^{-1})^7 are (4) 4×10^9, (3) 1×10^{10}, (2) 1.5×10^{10} and (1) 2×10^{10}. (C) Relationships for constant K_4 and K_8 but varying K_{16}; $K_4 = 6 \times 10^4$ (ml mg^{-1})^3 and $K_8 = 2 \times 10^9$ (ml mg^{-1})^7. The symbols and values of K_{16} (ml mg^{-1})^{15} are (4) 8×10^{18}, (3) 1×10^{19}, (2) 3×10^{19} and (1) 5×10^{19}.

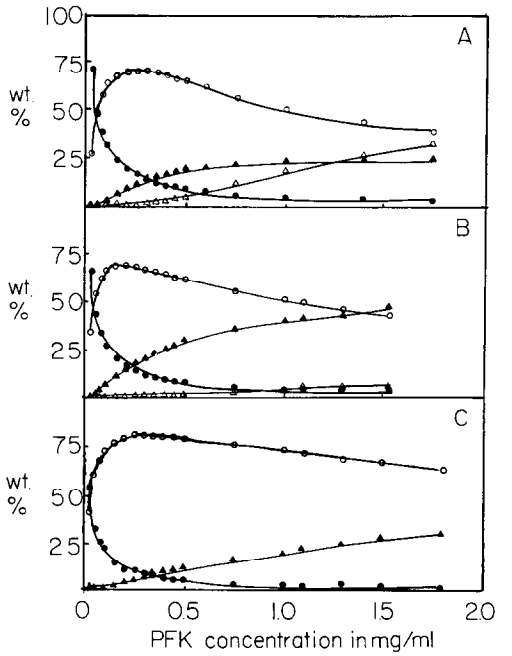

Fig. 3. (A), (B) Mass distributions of phosphorylated PFK and desphosphorylated PFK, respectively, among polymeric species in GKMED buffer as a function of the total protein concentration. ●, Monomer; ○, tetramer; ▲, octomer; Δ, hexadecamer. (C) Mass distribution of both forms of PFK in 3×TEMA buffer. ●, Monomer; ○, tetramer; ▲, octomer.

consistent with that from earlier studies [15,18], and they indicate that the binding of the substrate F6-P induces a quaternary structural change leading to a change in the sedimentation coefficients of the oligomeric forms of PFK. It is interesting to note that the presence of 0.2 mM F6-P does not alter the values for K_4 of either phosphorylated or dephosphorylated PFK, but a significant enhancement in K_8 and K_{16} is observed in both forms of PFK.

In the presence of 10 mM citrate, a significant amount of dimer is observed. For the dephosphorylated form, the values for K_2 and K_4 are larger and smaller, respectively, than the corresponding equilibrium constants for the phosphorylated PFK. The weight per cent distribution of various species in 10 mM citrate is shown in Fig. 4A and 4B. It is interesting to note that at the same protein concentration, the weight percent of dimer is significantly higher for dephosphorylated than for phosphorylated

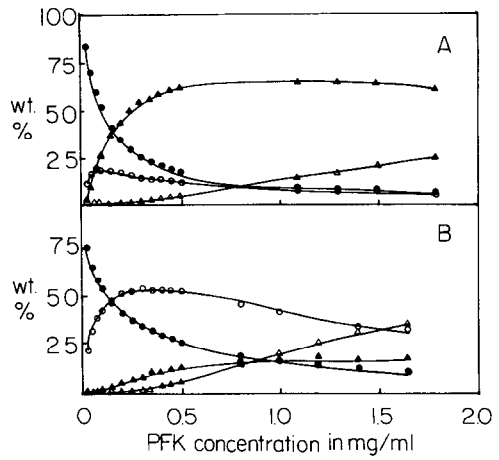

Fig. 4. (A), (B) Mass distributions of phosphorylated and dephosphorylated PFK, respectively, among polymeric species in 10 mM citrate–TEMA buffer as a function of the total protein concentration. ●, Monomer; ○, dimer; ▲, tetramer; Δ, octomer.

PFK. These results imply that the dephosphorylated form of PFK would be more susceptible to inhibition by citrate since the dimer is inactive.

Having analyzed the sedimentation data for the modes of association and equilibrium constants, it is useful to have a means of correlating the conclusions derived from this study with data reported in the literature. This might be accomplished by comparing the Schlieren or derivative sedimentation profiles. Gilbert and Gilbert [27] have proposed an elegant approach for comparing the theoretical sedimentation patterns with experimental velocity profiles. Subsequently, Frigon and Timasheff [28] have demonstrated the analytical power of such an approach in their study of calf brain tubulin self-association. In an effort to provide verification of the sedimentation results, sedimentation velocity profiles were calculated by using a program adopted from the method developed by Cox [29–33].

Based on the mode of association and equilibrium constants, the simulation program can calculate and describe the relationship between the weight-average sedimentation coefficient and the protein concentration. A similar dependence can also be calculated for diffusion. The values of the diffusion coefficients of the ith associating species were estimated from the Svedberg equation, using the S_i° values reported previously [26] and $\bar{v}$ of 0.730 [15]. Having generated the concentration dependences of $\overline{S}$ and $\overline{D}$ (weight-average diffusion coefficient), the numerical procedure of Cox [32,33] was applied to generate a protein concentration gradient in a hypothetical compartmentalized sector-shaped centrifuge cell. The results are displayed as a profile of concentration gradient as a function of radial distance from the center of rotation. A typical set of profiles is shown in Fig. 5 as a function of two protein concentrations. Bimodal sedimentation profiles are observed in contrast to the trimodal patterns reported in the literature.

The activating effect of F-actin on the PFK activity may conceivably be due to an enhanced self-association of PFK subunits. In order to define the role of F-actin, experiments were conducted to monitor PFK subunit interaction in the presence of F-actin. Sedimentation velocity studies on the self-association of PFK in the presence of F-actin are difficult to interpret. However, the two systems, i.e. actin and PFK, are linked by virtue of thermodynamic reciprocity in the intermolecular interaction as shown in the following scheme.

$$\begin{array}{ccccc} & & K_1 & & K_2 \\ E_1 & \rightleftarrows & E_4 + A_n & \rightleftarrows & nA \\ & & \Updownarrow K_3 & & \\ & & E_4A_n & & \end{array}$$

where E_1 and E_4 are monomeric and tetrameric forms of PFK, A and A_n are monomeric and poly-

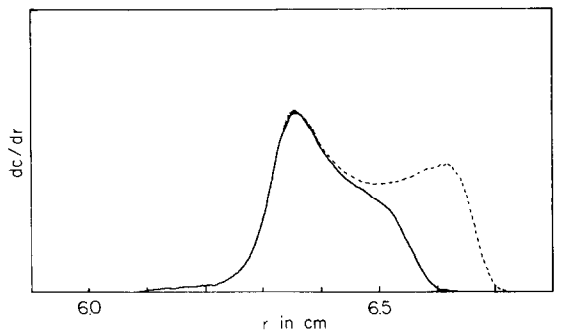

Fig. 5. Simulated sedimentation velocity profiles of phosphorylated PFK as a function of the protein concentration in TEMA buffer using the following parameters: $K_4 = 4.6 \times 10^5$ (ml mg^{-1})^3, $K_8 = 1.1 \times 10^{10}$ (ml mg^{-1})^7, $K_{16} = 7.8 \times 10^{22}$ (ml mg^{-1})^{15}. (Speed, 52000 rev min^{-1}; sedimentation time, 1663.5 s.) The total protein concentrations are (solid line) 500 μg ml^{-1} and (dotted line) 750 μg ml^{-1}.

meric forms of actin, and K_i are the various equilibrium constants characterizing these linked equilibria. Hence, the self-assembly of F-actin was monitored in the presence and absence of phosphorylated PFK. The results of turbidity measurements show that in the absence of PFK, self-assembly of F-actin occurs with a critical concentration of 0.78 mg m^{-1}, as shown in Fig. 6. The critical concentration corresponds to an apparent equilibrium constant K_p^{app}, of 5.5×10^4 l mol^{-1} and an apparent standard free energy change for the addition of a subunit to F-actin of $\Delta G^\circ_{app} = -6.1$ Kcal mol^{-1}. In a similar experiment in the presence of 0.2 mg ml^{-1} phosphorylated PFK, the F-actin self-assembly reaction is characterized by a critical concentration of 0.36 mg ml^{-1} as shown in Fig. 6. This critical concentration corresponds to K_p^{app} of 1.20×10^5 l mol^{-1} and ΔG°_{app} of -6.6 Kcal mol^{-1}. These results indicate that the ability of actin to self-assemble into F-actin is enhanced by the presence of 0.2 mg ml^{-1} of phosphorylated PFK to the extent of -0.5 Kcal mol^{-1} of actin. Due to the principle of thermodynamic reciprocity (see Ref. [34]), and assuming that tetrameric PFK binds more favorably to F-actin, i.e. insignificant interaction between monomeric actin and PFK of any state and of monomeric PFK with F-actin, the self-assembly of PFK must be enhanced to the same extent since

$$\Delta G^\circ_{(A)} + \Delta G^\circ_{(EA)} = \Delta G^\circ_{(E)} + \Delta G^\circ_{(AE)} = \Delta G^\circ_{AE} \qquad (2)$$

where $\Delta G^\circ_{(A)}$ and $\Delta G^\circ_{(E)}$ are the free energy changes of the subunit assembly for actin and PFK, respectively, $\Delta G^\circ_{(AE)}$ and $\Delta G^\circ_{(EA)}$ are the free energy changes

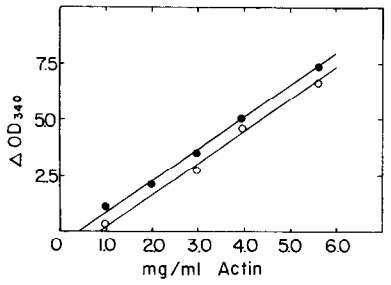

Fig. 6. Effect of actin concentration on the turbidity at 10°C. The solvent was 65 μM glycylglycine, 15 mM $MgCl_2$, 10 mM KCl, 1 mM EDTA, and 1 mM DTT at pH 7.0. The turbidity values are those observed in the plateau regions. ○, No PFK; ●, 0.2 mg ml^{-1} of PFK.

of actin and PFK assembly in the presence of PFK and actin, respectively, and ΔG°_{AE} designates the coupling free energy change in the formation of the PFK–F-actin complex from PFK and actin. In the context of this study, ΔG°_{AE} assumes a negative value, indicating that actin should exhibit a reciprocal effect in enhancing the self-association of PFK. Hence, it may be concluded that F-actin enhances the self-association of PFK, although this may not be the only effect that F-actin can exert on PFK. A consequence of enhanced self-association is a change in steady-state kinetic parameters as a function of the protein concentration. Such is indeed the case as reported by Luther and Lee [8].

4. Discussion

The results from this study demonstrated quantitatively that phosphorylation of rabbit muscle PFK can affect the propensity of PFK subunit self-assembly under some particular experimental conditions, e.g. phosphorylated PFK exhibits a fivefold lower K_4 value in GKMED buffer than in any of the other buffer systems studied in this laboratory. On the other hand, dephosphorylated PFK seems to be less sensitive to the same set of experimental changes, since the K_4 value is not changed more than threefold. Metabolites, particularly citrate, exert a differential effect on the propensity of these two forms of PFK to aggregate. Having demonstrated the effect of post-translational modification on the solution behavior of PFK, it would be useful to establish a correlation between the site of phosphorylation and subunit contacts. At present there is no information on the three-dimensional structure of rabbit muscle PFK, although Poorman et al. [35] have proposed a model of folding and subunit contacts based on the amino acid sequence of the rabbit muscle enzyme and the crystallographic information available for the bacterial enzyme. The proposed model indicates that the carboxyl terminus of each subunit is located at the external, away from the interface of subunits in the tetrameric state. Since the major known phosphorylation site has been reported to be a serine residue located at the sixth residue from the carboxyl terminus of the polypeptide, then it is conceivable that the phosphorylation site is exposed and removed from

the intersubunit interface. If that proved to be so, then phosphorylation apparently exerts long-range influence on the structure of muscle PFK, leading to a change in the energetics involved in intersubunit contacts.

The mode of association remains the same regardless of the state of phosphorylation. Under these experimental conditions, it could be best described as a system undergoing rapid dynamic equilibration with a stoichiometry of $M_1 \rightleftharpoons M_4 \rightleftharpoons M_8 \rightleftharpoons M_{16}$. Having established the differential sensitivity of the phosphorylated and dephosphorylated forms of PFK toward the experimental conditions, it is useful to examine these observations with respect to the literature. Many groups of workers have examined the sedimentation behavior of highly and poorly phosphorylated fractions of PFK [21,36,37]. The experimental conditions employed by these studies are different; hence, it is difficult to establish any quantitative correlation among them. However, a common conclusion of these studies is that the sedimentation profile is a function of the state of phosphorylation. At present, there are reports of apparently conflicting results [21,36,37]. Using PFK fractions of highly and poorly phosphorylated forms, Hussey et al. [36] conducted sedimentation studies, and the results showed that the highly phosphorylated fraction apparently has a lower tendency for aggregation showing only sedimentation components of 13*S* and 18*S*, whereas the lowly phosphorylated fraction contains a 30*S* component. These results imply that the dephosphorylated form of PFK may have a higher tendency to aggregate. In the meantime, Uyeda et al. [37] reported that, depending on the solvent compositions, the highly and lowly phosphorylated fractions of PFK may actually exhibit opposite tendencies to aggregate, i.e. the highly phosphorylated fractions may exhibit a higher content of aggregates in one case but less in the other. Foe and Kemp [22] reported no differences between the sedimentation behavior of the phosphorylated and dephosphorylated forms of PFK. These reported differences may be the consequence of studying a heterogenous population of PFK with different affinities for aggregation, or these results reflect the basic behavior of PFK in response to the differences in solvent compositions employed in these studies, or a combination of both factors. In an effort to determine, at a qualitative level, whether results obtained from this study could serve as a basis for the literature observation, a further simulation was conducted. A trimodal sedimentation profile can be generated with a stoichiometry of $M_1 \rightleftharpoons M_4 \rightleftharpoons M_8 \rightleftharpoons M_{16}$ with $K_4 = 1 \times 10^4$ (ml $mg^{-1})^3$, $K_8 = 1 \times 10^8$ (ml $mg^{-1})^7$, and $K_{16} = 6 \times 10^{18}$ (ml $mg^{-1})^{15}$, as shown in Fig. 7A. Increasing values of K can yield a sedimentation profile that is still trimodal but with significant change in the position and height of peaks, as shown in Fig. 7A. It is conceivable that by altering the magnitudes of these equilibrium constants, a set of equilibrium constants may generate sedimentation profiles that resemble those reported in the literature. Hence, the changes in areas under each peak are reflections of the changes in equilibrium constants depending on the phosphorylation state of the enzyme and the sensitivity of these multiple equilibria on specific solution conditions. Furthermore, the reported sedimentation profiles are results from studies using heterogenous PFK samples of phosphorylated and dephosphorylated forms. Hence, these profiles are most likely to be composites. An attempt was made to generate a composite profile for a 1:1 mixture of a PFK sample, as shown in Fig. 7A. The composite profile resembles the trimodal sedimentation patterns reported in the literature which show a series of inseparable peaks of increasing peak height and sedimentation coefficient (e.g. Fig. 3B in Ref. [36]). These same authors have also reported a sedimentation profile that shows three peaks, with the middle one exhibiting the greatest peak height. A composite profile that resembles the literature pattern can be generated, as shown in Fig. 7B. Therefore, a significant contribution of this study is to show that the apparently contradictory reported sedimentation behavior of PFK can be explained by a single mode for PFK assembly. These different sedimentation profiles are possibly the net results of differential responses of PFK of different phosphorylated states to the experimental conditions.

Similar conclusions can be derived from studies of the effects of metabolites in the subunit assembly of PFK. Based on the results from this study, one may predict that PFK will be equally activated by F6-P, regardless of the state of phosphorylation, while the dephosphorylated form would be more affected by citrate. These predicted results are differ-

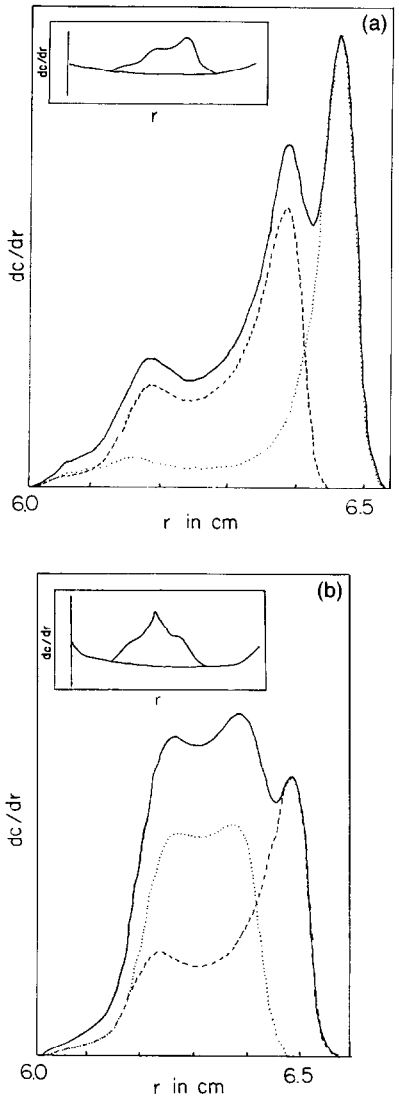

Fig. 7. Simulated sedimentation velocity profiles of PFK. (A) (· · ·) $K_4 = 1 \times 10^4$ (ml mg^{-1})^3, $K_8 = 1 \times 10^8$ (ml mg^{-1})^7 and $K_{16} = 6 \times 10^{18}$ (ml mg^{-1})^{15}; (---) $K_4 = 5 \times 10^4$ (ml mg^{-1})^3, $K_8 = 1 \times 10^9$ (ml mg^{-1})^7 and $K_{16} = 6 \times 10^{19}$ (ml mg^{-1})^{15}; (————), composite of a 1:1 mixture. (Protein concentration, 1.0 mg ml^{-1}; rotor speed, 52000 rev min^{-1}; simulation time, 961 s.) Insert: a tracing of Fig. 3B of Hussey et al. [36]. (B) (· · ·) $K_4 = 5 \times 10^4$ (ml mg^{-1})^3, $K_8 = 1 \times 10^9$ (ml mg^{-1})^7 and $K_{16} = 6 \times 10^{18}$ (ml mg^{-1})^{15}; (---) $K_4 = 5 \times 10^4$ (ml mg^{-1})^3, $K_8 = 1 \times 10^9$ (ml mg^{-1})^7 and $K_{16} = 6 \times 10^{19}$ (ml mg^{-1})^{15}; (————), composite of a 1:1 mixture. The protein concentration, rotor speed and simulation time were the same as in (A). Insert: a tracing of Fig. 3C of Hussy et al. [36].

ent from the literature results, in which no consistent pattern can be derived. Kemp and co-workers [22,38] reported that the dephosphorylated form of PFK exhibits hyperbolic kinetic behavior and is less inhibited by citrate, while the phosphorylated form exhibits sigmoidal kinetic behavior. Uyeda et al. [37] reported that there is no significant difference in the kinetic behavior between the two forms, although they show a significant difference in their sensitivity towards inhibitors. In the meantime, Hussy et al., [36] showed that there is no significant difference in the allosteric behavior between the highly and lowly phosphorylated fractions of PFK. Since this study has shown that the propensity of subunit assembly can be affected differently by solvent conditions and the phosphorylation state of the enzyme, it is not surprising that there is no consistent conclusion on the kinetic behavior of PFK. All these studies were conducted under different solvent conditions and it is conceivable that these apparently contradictory results are simply the consequences of differential perturbation of various equilibria that are linked in an intricate fashion to control the activity of PFK.

In summary, this study provides a plausible rationale to account for the apparently different observations reported in the literature. These results re-emphasize the fact that allosteric systems are controlled by networks of intricate linked reactions. In the PFK system, the intricate network includes at least the binding affinities of ligands to the various oligomeric forms. The minimum number of ligands include two substrates, one inhibitor and one activator. Furthermore, there may be additional site–site interactions between these sites. An understanding of the ground rules which govern this allosteric system requires a systematic dissection of these linked reactions.

Acknowledgements

This paper is dedicated to the celebration of the 10th anniversary of the Gibbs Conference on Biothermodynamics. JCL wishes to acknowledge the special contribution of the late Stanley J. Gill in initiating this conference. The study was supported

by NIH grant GM-45579 and the Robert A. Welch Foundation grants H-0013 and H-1238.

References

[1] P. Sigel and D. Pette, J. Histochem. Cytochem., 17 (1969) 225.
[2] G. Doeken, E. Leisner and D. Pette, Histochemistry, 43 (1975) 113.
[3] T. Keleti, J. Ovadi and J. Batke, Prog. Biophys. Mol. Biol., 53 (1989) 105.
[4] D.K. Srivastava and S.A. Bernhard, Curr. Top. Cell. Regul., 28 (1986) 1.
[5] D.K. Srivastava and S.A. Bernhard, Ann. Rev. Biophys. Chem., 16 (1987) 175.
[6] H. Arnold, R. Henning and D. Pette, Eur. J. Biochem., 22 (1971) 121.
[7] F.M. Clarke and C.J. Masters, Biochim. Biophys. Acta, 381 (1975) 37.
[8] M.A. Luther and J.C. Lee, J. Biol. Chem., 261 (1986) 1753.
[9] H.-J. Kuo, D.A. Malencik, R.-S. Liou and S.R. Anderson, Biochemistry, 25 (1986) 1278.
[10] S.J. Roberts and G.N. Somero, Biochemistry, 26 (1987) 3437.
[11] T.P. Walsh, D.J. Winzor, F.M. Clarke, C.J. Masters and D.J. Morton, Biochem. J., 186 (1980) 89.
[12] T.P. Walsh, C.J. Masters, D.J. Maston and F.M. Clarke, Biochem. Biophys. Acta, 675 (1981) 29.
[13] F.M. Clarke, F.D. Shaw and D.J. Morton, Biochem. J., 186 (1980) 105.
[14] R.S. Liou and S. Anderson, Biochemistry, 19 (1979) 2684.
[15] L.K. Hesterberg and J.C. Lee, Biochemistry, 20 (1981) 2974.
[16] L.K. Hesterberg and J.C. Lee, Biochemistry, 21 (1982) 216.
[17] P.M. Lad, P.E. Hill and G.G. Hammes, Biochemistry, 12 (1973) 4303.
[18] M.A. Luther, H.F. Gilbert and J.C. Lee, Biochemistry, 23 (1983) 5494.
[19] M.A. Luther, L.K. Hesterberg and J.C. Lee, Biochemistry, 24 (1985) 2463.
[20] J.C. Lee, L.K. Hesterberg, M.A. Luther and G.-Z. Cai, in G. Herve (Ed.), Allosteric Enzymes, CRC Press, Florida, 1989, p. 231.
[21] S. Kitajima, R. Sakakibara and K. Uyeda, J. Biol. Chem., 258 (1983) 13292.
[22] L.G. Foe and R.G. Kemp, J. Biol. Chem., 257 (1982) 6368.
[23] H. Hasegawa, M. Parniak and K. Seymour, Anal. Biochem., 120 (1982) 360.
[24] F. Gaskin, C.R. Cantor and M.L. Shelanski, J. Med. Biol., 89 (1974) 737.
[25] F. Oosawa and M. Kasai, Biol. Macromol., 5 (1971) 261.
[26] G.-Z. Cai, L.L.-Y. Lee, M.A. Luther and J.C. Lee, Biophy. Chem., 37 (1990) 97.
[27] L.M. Gilbert and G.A. Gilbert, Methods in Enzymol., 27 (1973) 273.
[28] R.P. Frigon and S.N. Timasheff, Biochemistry, 14 (1975) 4559.
[29] D.J. Cox, Arch. Biochem. Biophys., 119 (1967) 230.
[30] D.J. Cox, Arch. Biochem. Biohys., 129 (1967) 106.
[31] D.J. Cox, Arch. Biochem. Biophys., 142 (1971) 514.
[32] D.J. Cox, Methods in Enzymol., 48 (1978) 212.
[33] D.J. Cox and R.S. Dale, in C. Frieden and L.W. Nichol (Eds.), Protein–Protein Interactions, Wiley–Interscience, New York 1981, p. 172.
[34] G. Weber, Adv. Protein Chem., 29 (1975) 1.
[35] R.A. Poorman, A. Randolph, R.G. Kemp and R.L. Heinriksen, Nature, 309 (1984) 467.
[36] C.R. Hussy, P.F. Liddle, D. Ardron and G.L. Kellett, Eur. J. Biochem., 80 (1977) 497.
[37] K. Uyeda, A. Miyatake, L.J. Luby and E.G. Richards, J. Biol. Chem., 253 (1978) 8319.
[38] R.G. Kemp, L.G. Foe, S.P. Latshaw, R.A. Poorman and R.L. Heinrikson, J. Biol. Chem., 256 (1981) 7282.